

# Experimental investigation of novel gas turbine film cooling configuration using phosphor thermometry

G. Lalizel<sup>1\*</sup>, A. Subramanian, P. Berterretche<sup>1</sup> and E. Dorignac<sup>1</sup>

1: Institut P' – CNRS UPR 3346 / ISAE-ENSMA & University of Poitiers 1, Av Clément Ader, 86360 Chasseneuil du Poitou, FRANCE.

\* Corresponding author: gildas.lalizel@ensma.fr

## Abstract

Film cooling techniques have been extensively employed to improve the turbine inlet temperatures so as to improve the efficiency of a gas turbine engine. This article presents experimental instantaneous 2D temperature fields analysis obtained with ZnO phosphorescence for M blowing ratio equal to 3, on BATH test-rig.

**Keyword:** Film cooling, phosphor thermometry, Jet in crossflow

## 1. Introduction

In the recent times, there is an increased emphasis on reducing the gaseous emissions, especially in the aviation sector. In this regard, the gas turbine engine cycle efficiencies are required to be at their highest so as to reduce the fuel consumption and hence the emissions. In the quest for higher working efficiency, cooling strategies have been employed in the combustion chamber and the turbine blades so as to improve the Turbine Inlet Temperature (TIT), due to the fact that combustion at higher temperatures yield higher efficiency. One of the cooling strategies currently in use is film cooling, which employs a film of air covering the surface to be cooled so as to reduce the heat transfer into the surface, turbine blade for example. Over the years various studies have been conducted to study the effect of hole shapes, arrangement of holes, density ratio, blowing ratio, and other factors [3].

Film cooling applications involve a phenomena called the Jet in cross flow (JICF) where a coolant jet is injected across a wall into a mainstream flow. Such a flow is observed in many other cases like a chimney or volcanic eruption too. The aerodynamic consequences due to the interaction of the jet with the cross-flow are many and it is important to understand the flow structures that evolve around the jet. Figure 1 shows a classical JICF arrangement.

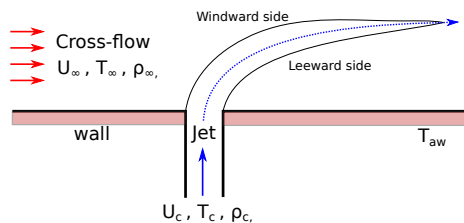


Fig. 1: Arrangement of a Jet In Cross-Flow system.

In the recent past, improvements in additive manufacturing and the improvements in precision engineering have paved the way to make finer and complex hole shapes. The shape of the hole and its characteristics like the channel angle, hole exit angle, orientation of the hole with respect to the axis of the crossflow have a profound effect on the flow structures downstream of the hole exit. Various complex hole shapes have been proposed and analysed (Fan shaped by [6], ramp by [2], slot cooling by [11], effusion cooling by [8]) other

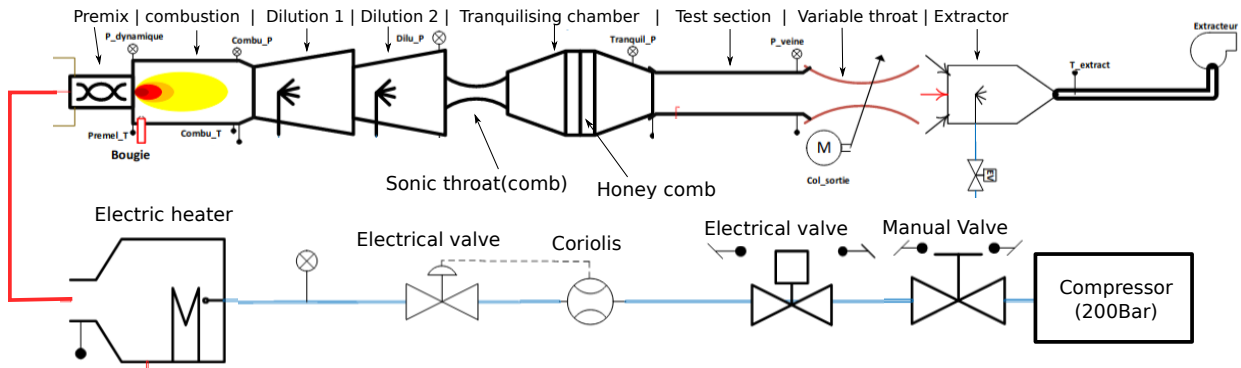


Fig. 2: Schematic view of the Bath test rig components

than usual cylindrical hole shapes ([9],[13]) with the aim to improve the film cooling efficiency through reduction in the CRVP intensity and height. Despite this, primitive hole shapes are preferred so as to reduce the manufacturing costs involved in producing complex shapes and to facilitate easier maintenance of the turbine blades once in service.

The system of a cylindrical hole with auxiliary holes or 'sister holes' arrangement was proposed in the 2000s by [7]. Since then few number of numerical studies have been done on such an arrangement where a main hole is supported by two smaller holes upstream or downstream ([5],[4], [10]). The understanding from these works is that the efficiency of the sister hole arrangement is improved immensely comparing with a simple single hole geometry. However, since most of the studies are numerical analyses alone, there is a need for experimental test data. In this article, phosphor thermometry is employed to test this novel hole arrangement so as to visualise the 2-D temperature field.

### 1.1. Objectives of this study

This work aims to establish the working of the auxiliary hole film cooling configuration which has the potential to improve film cooling efficiency without requiring much improvements in machining techniques.

- Phosphor thermometry using ZnO particles set-up to visualise the 2-D temperature flow fields in film cooling arrangements.
- Study the flow fields in a simple cylindrical hole arrangement and auxiliary hole arrangement along the flow direction and the spanwise direction.
- Instantaneous and average temperature flow-field data.

## 2. Experimental setup

### 2.1. Description of test bench

The BATH test bench is an open circuit wind tunnel which aims to recreate the flow and temperature conditions found in aero engines within a test section. Air from a compressor tank is electrically heated before controlled air-kerosene combustion which raises the temperature of the air to extreme temperatures.

The boundary conditions of the film cooling arrangement are shown in table 1. Electrically heated air at 150°C is fed in the crossflow at a mass flow rate of 300g/s. A seeding chamber helps in infusing ZnO phosphor particles in the flow. Film cooling holes are connected to a separate seeding chamber which is fed with a constant mass flow rate of 4.45g/s thanks to an orifice tube which ensures constant a mass flow rate. This air is maintained at 20°C, which leads to a blowing ratio of  $M=3$ . The reason for choosing a higher blowing ratio is the high jet penetration, which makes the visualisation of the 2-D temperature field all along the jet trajectory achievable. Additionally, the coherent structures are amplified and helps in better identification and quantification.

### 2.2. Film cooling geometry

In this section, the film configurations are described. In order to have preliminary verification that the proposed auxiliary hole configurations have favourable flow characteristics, a case with cylindrical hole is used as a reference. Table 2 shows the various geometrical characteristics of the two configurations studied.

Tab. 1: Boundary conditions

Parameter	Cross-flow	Jet
Mass flow	310g/s	4.45g/s
Temperature	150°C	20°C
Density	0.83kg/m <sup>3</sup>	1.32kg/m <sup>3</sup>
Pressure	1.2bar	1.2bar
Velocity (theoretical)	12.8m/s	27.5m/s
Blowing ratio 'M'	3	
Density ratio	1.45	

Tab. 2: Geometric parameters

Parameter	Single hole	Aux. hole case
Main hole Diameter	$D_1=12.25$ [mm]	$D=10$ [mm]
Aux. hole Diameter	-	$d=5$ [mm]
Aux. hole lateral distance	-	$H=15$ [mm]
Aux. hole longitudinal distance	-	$L=15$ [mm]

### 3. Phosphor thermometry setup

The use of phosphor thermometry is a novelty in analysing the film cooling physics in this work. A short description of the spectral intensity ratio method and the properties of ZnO phosphor are presented. Additionally, an overview of the various components necessary to acquire the images are described in this section. A more detailed explanation is provided in a separate article on ZnO phosphor thermometry [12].

#### 3.1. Spectral intensity ratio method

The phosphor particles absorb the incident radiation  $I_0$  and get excited to higher temporary energy states. They return to the lower energy states by emission of radiation, and for the purpose of phosphor thermometry, phosphors with emission in the visible spectrum are preferred. The number of photons emitted upon excitation by a laser depends on various factors like temperature of the working fluid  $T$ , the local concentration  $\chi$  of particles, the laser sheet intensity  $I_0$  working at wavelength  $\lambda_0$  and the inherent emission property of the phosphor used  $\sigma$ . The emission intensity  $I$  is given by the expression:

$$I(\lambda, x, y, z) \approx \underbrace{I_0(\lambda_0, x, y, z)}_{(1)} \underbrace{\sigma(\lambda_0, T)}_{(2)} \underbrace{\exp(-\chi(x, y, z)d)}_{(3)} \underbrace{\chi(x, y, z)}_{(4)} \quad (1)$$

In the above equation the emission intensity hence depends on (1) laser wavelength and intensity, (2) phosphor characteristics, (3) the local absorption due to Beer-Lambert effect and (4) local concentration of phosphor particles. In addition to these parameters, factors like detector efficiency, the transitivity of optics and the direction at which the radiation is emitted upon excitation also play a role on the detected emission intensity.

By observing the phosphor emission through two different wavelength bandwidths by use of filters, the division of the two filtered images can be effectively used to calibrate temperatures. However, due to the use

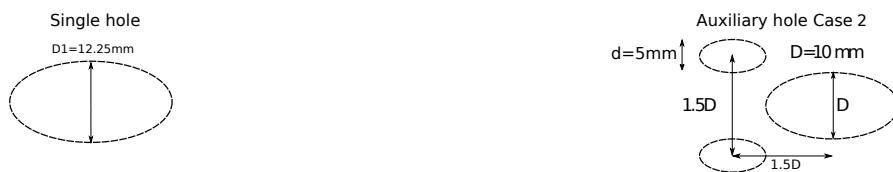


Fig. 3: Hole shape from the top view is shown below each module with geometrical parameters.

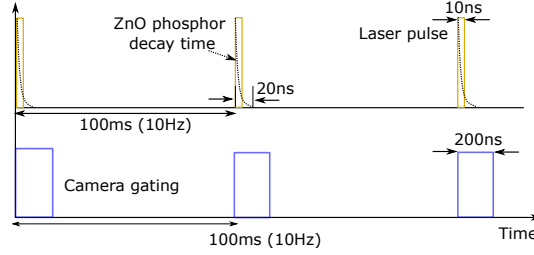


Fig. 4: Timing and synchronisation diagram showing the camera and laser firing.

of filters, the collection of the emission signal is drastically reduced, and sometimes necessitates the need for an intensified camera.

As the spectroscopic distribution changes, the relative intensity of some of the emission bands varies in relation to one another. By collecting the emission intensity of each of the two bands by means of a 2-D detector, such as an ICCD camera, the intensity ratio at a specific temperature can be obtained. By changing the temperature of the phosphor, full temperature calibration of this ratio can be achieved.

From eq. 1 it can be seen that the emission dependence on the laser wavelength, local Beer-Lambert absorption and the local concentration of the particles can be eliminated, if the intensity of emission emitted by a phosphor particle at different wavelengths can be divided by one another.

$$\frac{S_{\lambda_1}}{S_{\lambda_2}} = \frac{\sigma(\lambda_0, T_1)}{\sigma(\lambda_0, T_2)} \quad (2)$$

From eq. 2, it can be seen that by such a division, the intensity ratio value depends only on the temperature of the phosphor and the excitation source wavelength.

There are several setup configurations that can be used to determine temperatures by use of the intensity ratio method. The first of these involves use of two cameras, each equipped with an interference filter that transmits one of the bands of the emitted radiation and blocks the others. This configuration requires spatial matching of the two detectors in order to obtain an accurate two-dimensional temperature map. The second configuration utilizes a stereoscope fitted to a single camera, which enables the projection of the spectral intensity of each band onto a single detector chip. Stereoscopes can suffer from radiation cross-talk, which can affect the accuracy of the temperature determination obtained though.

### 3.1.1. Other components

A Quantel Q-smart 850 laser, operating at 10 Hz with a 6 ns pulse duration and an energy output of 100 mJ (energy density of 50 mJ/cm<sup>2</sup>), was used for PIV analysis and phosphor thermometry, sufficient for luminescence emission in the saturated regime. The ANDOR iStar sCMOS camera, with an intensifier and short gating width (200 ns), captured high-resolution images of the flow field. For each calibration point and film cooling case, 150 images were acquired at 10 Hz with a camera gain of 2000. The experimental setup included relay mirrors to direct the 266 nm laser beam to a sheet generator, producing a laser sheet thinner than 0.5 mm. This configuration helped minimize three-dimensional particle effects in the flow, and an Optosplit II device enabled spectral intensity ratio imaging with a single camera. Figures 4, ?? illustrate the timing, setup, and laser path, as well as raw image outputs from the experiments.

The Optosplit is used to separate incident emission radiation from the ZnO into two paths, with each passing through a bandpass filter: ET395/25x and AT425/50x. After passing through the filters, these two paths are 're-parallelled' to form two images of the same region of interest on the same image frame. A larger bandwidth for the filters was selected than the previous studies [1] to allow more incident light on the camera.

### 3.2. Calibration

The calibration procedure starts with the acquisition of the intensity images of the two spectral bands that have been pre-selected by the user. Then, the images are subjected to background subtraction and to de-warping process to adjust image distortions. After this the division of the two intensity maps results in the intensity ratio distribution corresponding to the temperature distribution of the object. The intensity

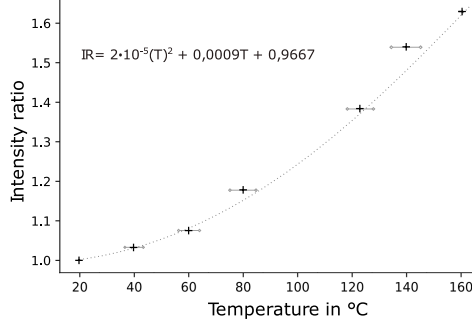


Fig. 5: Intensity ratio vs temperature calibration curve for the ZnO phosphor in air.

ratio distribution obtained is then transformed into temperature values by use of a calibration polynomial to convert the ratios obtained.

At least 7 calibration points were chosen to obtain the intensity ratio vs temperature calibration curve as shown in the figure 5. The images acquired were applied with a moving Gaussian filter (3x3 pixels) and binned (5x5 pixels) using python code developed in-house.

#### 4. Results

Both the configuration were tested at a blowing ratio of 3 owing to the simplicity in capturing the flow field far away from the wall. This is preferred as the ZnO particle deposition on the walls can cause bright zones just above the wall which lead to non-physical results. Low blowing ratio flows are restricted to short heights over the wall and hence limit the visualisation. In this section, the 2-D temperature visualisation results are presented for the baseline case (single hole case) and the auxiliary hole case. The 2-D non-dimensional temperature ( $\theta$ ) fields obtained from the film cooling experiments are discussed.

$$\theta = \frac{T_{\infty} - T}{T_{\infty} - T_c} \quad (3)$$

##### 4.1. Single hole configuration

Figures ??show the 2-D non-dimensional temperature fields for the single hole case at  $Y/D=0$ . The regions marked in blue indicate the presence of jet flow and the regions marked in red indicate mainstream flow and any color in between highlights the mixing between the jet and mainstream flows. In figure 6, (a) shows the mean flow field and (b-d) show the instantaneous flow field obtained. From 6(a), one can clearly observe the trajectory of the film cooling jet as well as the prominent  $\theta$  contours. The jet penetrates into the mainstream flow and has enough momentum to remain detached from the wall. In 6 (b), (c), (d) the instantaneous images help in identifying the jet-shear layer vortices in the top and the bottom areas of the jet. Additionally, it can be seen that the jet initially penetrates into the mainstream and later becomes unstable upon interaction with the main flow and 'packets' of cold air mix with the mainstream further downstream.

##### 4.2. Auxiliary hole configuration

The auxiliary hole case presents interesting 2-D temperature contour results. Figures 8 show the non-dimensional temperature contour as discussed earlier. (a) shows the mean flow field and (b-d) show the instantaneous flow field obtained at different instances. The first observation of figure 8 (a) highlights the tendency of the jet flow to be closer towards the wall than that of the single hole case ( refer figure 6 (a)). Similar to the single hole case, the jet flow throws out packets of cold air that mix with the main flow further downstream.

It is evident that the visualisation of the temperature flow field using phosphor thermometry is highly beneficial to the better understand of the film cooling process as it allows comparison between different film cooling configurations, and identification of coherent structures.

#### 5. Conclusion

In this article, the new BATH test rig where the film cooling study is conducted has been described. ZnO phosphor thermometry was successfully implemented to study film cooling configurations in this test

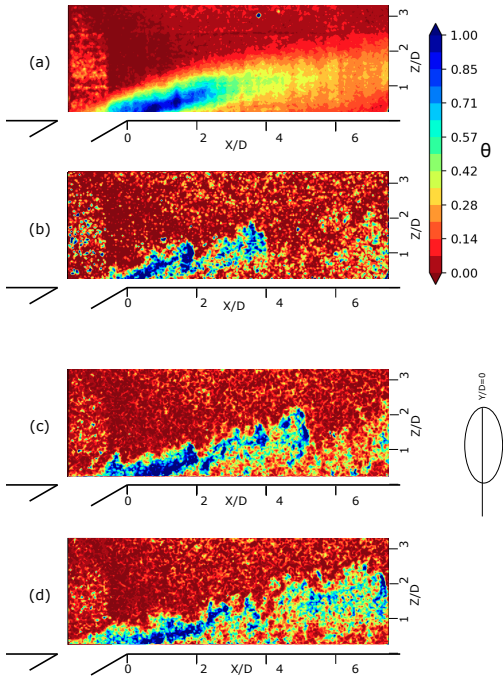


Fig. 6: Phosphor thermometry: Non-dimensional temperature contours for  $M=3$  for single hole case at  $Y/D=0$ . (a) Mean flow field. (b-d) instantaneous flow fields at different instances.

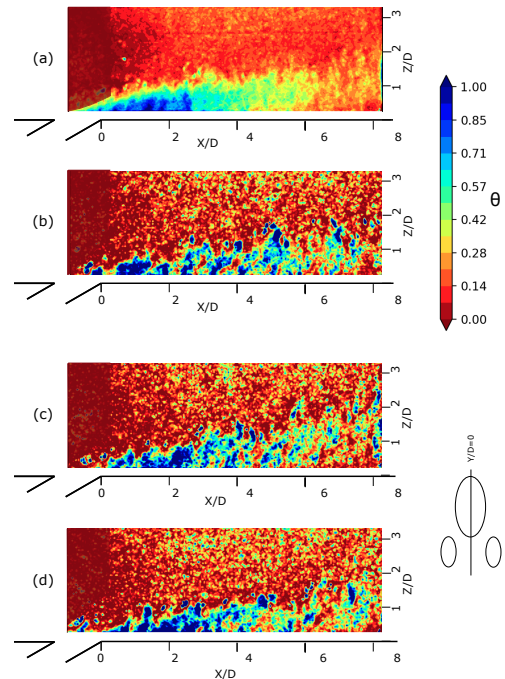


Fig. 7: Phosphor thermometry: Non-dimensional temperature contours for  $M=3$  for Auxiliary hole case at  $Y/D=0$ . (a) Mean flow field. (b-d) instantaneous flow fields at different instances.

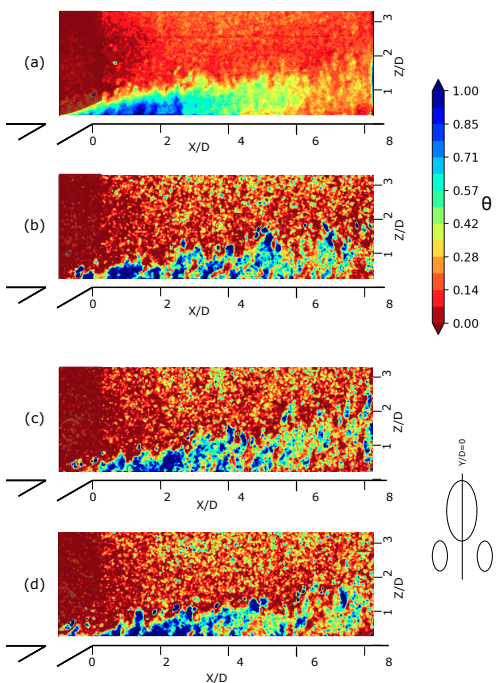


Fig. 8: Phosphor thermometry: Non-dimensional temperature contours for  $M=3$  for Auxiliary hole case at  $Y/D=0$ . (a) Mean flow field. (b-d) instantaneous flow fields at different instances.

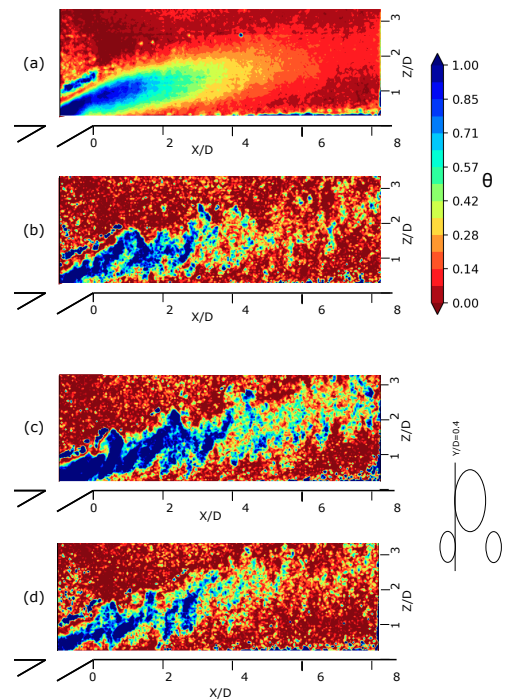


Fig. 9: Phosphor thermometry: Non-dimensional temperature contours for  $M=3$  for Auxiliary hole case at  $Y/D=0.4$ . (a) Mean flow field. (b-d) instantaneous flow fields at different instances.

bench. A cold jet seeded with ZnO particles was injected in a main seeded crossflow at 150°C with a blowing ratio  $M=3$ . This blowing ratio was used due to the better visualisation possible due to high penetration of the injected cold jet. High resolution 2-D temperature contour results were obtained through a series of experiments for the three test cases. The key learning from this study was that the auxiliary hole system has very favourable flow characteristics as compared to the single hole case, as the cold jet stays closer to the wall. Additionally, the injected jet in the auxiliary hole case has a greater lateral spread ( $Y/D_i 0.8$ ) than that of the single hole case ( $Y/D \approx 0.4$ ). The possibility of identifying key coherent structures like the jet-shear layer vortices show the fidelity of the phosphor thermometry technique. In order to understand these complex 3-D structures observed in experiments, Large Eddy Simulations can provide better insights.

### 6. Acknowledgements

This work was partially funded by the French Government program “Investissements d’Avenir” (EQUIPEX GAP, reference ANR-11-EQPX-0018).

### References

- [1] Christopher Abram, Miriam Pougin, and Frank Beyrau. “Temperature field measurements in liquids using ZnO thermographic phosphor tracer particles”. In: *Experiments in Fluids* 57.7 (2016), p. 115.
- [2] Giovanna Barigozzi, Giuseppe Franchini, and Antonio Perdichizzi. “The effect of an upstream ramp on cylindrical and fan-shaped hole film cooling: Part II—Adiabatic effectiveness results”. In: *Turbo Expo: Power for Land, Sea, and Air*. Vol. 47934. 2007, pp. 115–123.
- [3] Ronald S Bunker. “A review of shaped hole turbine film-cooling technology”. In: *J. Heat Transfer* 127.4 (2005), pp. 441–453.
- [4] Marc J Ely and BA Jubran. “A numerical study on improving large angle film cooling performance through the use of sister holes”. In: *Numerical Heat Transfer, Part A: Applications* 55.7 (2009), pp. 634–653.
- [5] Marc J Ely and BA Jubran. “A numerical study on increasing film cooling effectiveness through the use of sister holes”. In: *ASME Turbo Expo 2008: Power for Land, Sea, and Air*. American Society of Mechanical Engineers Digital Collection. 2008, pp. 341–350.
- [6] Michael Gritsch et al. “Effect of hole geometry on the thermal performance of fan-shaped film cooling holes”. In: (2005).
- [7] James D Heidmann and Srinath Ekkad. “A novel antivortex turbine film-cooling hole concept”. In: *Journal of turbomachinery* 130.3 (2008).
- [8] T Lenzi et al. “Time-Resolved Flow Field Analysis of Effusion Cooling System With Representative Swirling Main Flow”. In: *Journal of Turbomachinery* 142.6 (2020).
- [9] Ewald Lutum and Bruce V Johnson. “Influence of the hole length-to-diameter ratio on film cooling with cylindrical holes”. In: (1999).
- [10] Sehjin Park et al. “Design of sister hole arrangements to reduce kidney vortex for film cooling enhancement”. In: *Journal of Mechanical Science and Technology* 31.8 (2017), pp. 3981–3992.
- [11] JE Sargison et al. “A converging slot-hole film-cooling geometry—part 1: low-speed flat-plate heat transfer and loss”. In: *J. Turbomach.* 124.3 (2002), pp. 453–460.
- [12] Arunprasath Subramanian et al. “ZnO phosphor thermometry in water: Novel temporal method using rise time-decay time ratio”. In: *Measurement science and technology journal* 35 (2024).
- [13] Dibbon K Walters and James H Leylek. “A detailed analysis of film-cooling physics: part I—streamwise injection with cylindrical holes”. In: *J. Turbomach.* 122.1 (2000), pp. 102–112.